

Inhibition Effect of Cefradine on Corrosion of Mild Steel in HCl Solution

Ashish Kumar Singh^{1,2}, Aditya Kumar Singh³, Eno E. Ebenso^{1,2,*}

¹Department of Chemistry, School of Mathematical and Physical Sciences, North West University (Mafikeng Campus), Private Bag X2046, Mmabatho 2735, South Africa

²Material Science Innovation & Modelling (MaSIM) Research Focus Area, Faculty of Agriculture, Science and Technology, North-West University (Mafikeng Campus), Private Bag X2046, Mmabatho 2735, South Africa

³Department of Ceramic Engineering, Indian Institute of Technology, Banaras Hindu University, Varanasi, India-221 005

*E-mail: Eno.Ebenso@nwu.ac.za

Received: 8 September 2013 / *Accepted:* 2 November 2013 / *Published:* 15 November 2013

The corrosion inhibition properties of cefradine (CFD) for mild steel corrosion in HCl solution were analysed by electrochemical impedance spectroscopy (EIS), potentiodynamic polarization and gravimetric methods. Potentiodynamic polarization study clearly revealed that cefradine acted as mixed type inhibitor. The experimental data showed a frequency distribution and therefore a modelling element with frequency dispersion behaviour, a constant phase element (CPE) has been used. The various thermodynamic parameters of dissolution and adsorption processes were evaluated in order to elaborate adsorption mechanism. Adsorption of inhibitor obeyed Langmuir adsorption isotherm model.

Keywords: EIS; Acid solutions; Cefradine Mild steel; potentiodynamic polarization; acid inhibition

1. INTRODUCTION

Organic inhibitors were applied extensively to protect metals from corrosion in many aggressive acidic media (e.g. in the acid pickling and cleaning processes of metals) [1–3]. Organic compounds containing N, S and O atoms [4-11] were found to be good corrosion inhibitors of metals particularly for active metals like Fe, Zn, and Mg etc. The effectiveness of these compounds as corrosion inhibitors has been interpreted in terms of their molecular structure, molecular size, and molecular mass, hetero-atoms present and adsorptive tendencies [12]. Under certain conditions, the electronic structure of the organic inhibitors has a key influence on the corrosion inhibition efficiency

to the metal. The inhibitors influence the kinetics of the electrochemical reactions which constitute the corrosion process and thereby modify the metal dissolution in acids. The existing data show that most organic inhibitors act by adsorption on the metal surface. They change the structure of the electrical double layer by adsorption on the metal surface. Quite a number of studies have been carried out in determination of adsorptivity of various compounds at the electrode/solution interface [13-14].

A large number of organic compounds were studied as corrosion inhibitor, unfortunately most of the organic inhibitors used are very expensive and health hazards. Their toxic properties limit their field of application. Thus, it remains an important object to find cost-effective and non-hazardous inhibitors for the protection of metals against corrosion. Recently, a few non-toxic compounds such as diethylcarbamazine, tryptamine, succinic acid, L-ascorbic acid, sulphamethaxazole, cefatraxyl, disulfiram, ceftobiprole, cefuroxime, cefazolin, cefapirin, ceftazole etc. have been studied as corrosion inhibitors by our researchers [15-25].

This article reported our attempt to use electrochemical impedance spectroscopy (EIS), potentiodynamic polarization and weight loss method to investigate the nature of adsorption of cefradine on the mild steel surface. The structure of cefradine is shown in Figure 1.

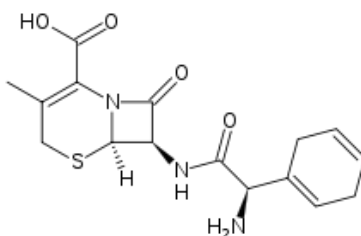


Figure 1. Structure of Cefradine molecule

2. EXPERIMENTAL

2.1 Inhibitor

Stock solution of cefradine was made in 10:1 ratio water: ethanol mixture to ensure solubility. This stock solution was used for all experimental purposes.

2.2 Corrosion measurements

Prior to all measurements, the mild steel specimens, having composition (wt %) C = 0.17, Mn = 0.46, Si = 0.26, S = 0.017, P = 0.019 and balance Fe, were abraded successively with emery papers from 600 to 1200 grade. The specimen were washed thoroughly with double distilled water, degreased with acetone and finally dried in hot air blower. After drying, the specimen were placed in desiccator and then used for experiment. The aggressive solution 1 M HCl was prepared by dilution of analytical grade HCl with double distilled water and all experiments were carried out in unstirred solutions. The

rectangular specimens with dimension $2.5 \times 2.0 \times 0.025$ cm were used in weight loss experiments and of size $1.0 \text{ cm} \times 1.0 \text{ cm}$ (exposed) with a 7.5 cm long stem (isolated with commercially available lacquer) were used for electrochemical measurements.

2.3 Electrochemical impedance spectroscopy

The EIS tests were performed at 303 ± 1 K in a three electrode assembly. A saturated calomel electrode was used as the reference; a 1 cm^2 platinum foil was used as counter electrode. All potentials are reported vs. SCE. Electrochemical impedance spectroscopy measurements (EIS) were performed using a Gamry instrument Potentiostat/Galvanostat with a Gamry framework system based on ESA 400 in a frequency range of 100000 Hz to 0.01 Hz under potentiodynamic conditions, with amplitude of 10 mV peak-to-peak, using AC signal at E_{corr} . Gamry applications include software DC105 for corrosion and EIS300 for EIS measurements, and Echem Analyst version 5.50 software packages for data fitting. The experiments were measured after 30 min. of immersion in the testing solution (no deaeration, no stirring). The working electrode was prepared from a square sheet of mild steel such that the area exposed to solution was 1 cm^2 .

The charge transfer resistance values were obtained from the diameter of the semi circles of the Nyquist plots. The inhibition efficiency of the inhibitor was calculated from the charge transfer resistance values using the following Eqn.

$$E\% = \frac{R_{\text{ct}}^i - R_{\text{ct}}^0}{R_{\text{ct}}^i} \times 100 \quad (1)$$

where R_{ct}^0 and R_{ct}^i are the charge transfer resistance in absence and in presence of inhibitor, respectively.

2.4 Potentiodynamic polarization

The electrochemical behaviour of mild steel sample in inhibited and non-inhibited solution was studied by recording anodic and cathodic potentiodynamic polarization curves. Measurements were performed in the 1 M HCl solution containing different concentrations of the tested inhibitors by changing the electrode potential automatically from -250 to +250 mV vs. corrosion potential at a scan rate of 1 mV s^{-1} . The linear Tafel segments of anodic and cathodic curves were extrapolated to corrosion potential to obtain corrosion current densities (I_{corr}).

The inhibition efficiency was evaluated from the measured I_{corr} values using the relationship:

$$E\% = \frac{I_{\text{corr}}^0 - I_{\text{corr}}^i}{I_{\text{corr}}^0} \times 100 \quad (2)$$

where, I_{corr}^0 and I_{corr}^i are the corrosion current density in absence and presence of inhibitor, respectively.

2.5 Linear polarization measurement

The corrosion behaviour was studied with polarization resistance measurements (R_p) in 1 M HCl solution with and without different concentrations of studied inhibitors. The linear polarization study was carried out from cathodic potential of -20 mV vs. OCP to an anodic potential of + 20 mV vs. OCP at a scan rate 0.125 mV s^{-1} to study the polarization resistance (R_p) and the polarization resistance was evaluated from the slope of curve in the vicinity of corrosion potential. From the evaluated polarization resistance value, the inhibition efficiency was calculated using the relationship:

$$E\% = \frac{R_p^i - R_p^0}{R_p^i} \times 100 \quad (3)$$

where, R_p^0 and R_p^i are the polarization resistance in absence and presence of inhibitor, respectively.

2.6 Weight loss measurements

Weight loss measurements were performed on rectangular mild steel samples having size $2.5 \times 2.0 \times 0.025 \text{ cm}$ by immersing the mild steel coupons into acid solution (100 mL) without and with different concentrations of isoniazid derivatives. After the elapsed time, the specimen were taken out, washed, dried and weighed accurately. All the tests were conducted in aerated 1 M HCl. All the experiments were performed in triplicate and average values were reported. From the evaluated weight loss, the surface coverage (θ) and inhibition efficiency ($E\%$) was calculated using:

$$\theta = \frac{w_0 - w_i}{w_0} \quad (4)$$

$$E\% = \frac{w_0 - w_i}{w_0} \quad (5)$$

where, θ is surface coverage, w_0 is weight loss in free acid solution and w_i is weight loss in acid solution in presence of inhibitor, respectively.

3. RESULTS AND DISCUSSION

3.1 Electrochemical impedance spectroscopy

The corrosion behaviour of mild steel in 1 M HCl in absence and presence of cefradine were investigated by EIS after immersion for 30 min at $303 \pm 1 \text{ K}$. Nyquist plots of mild steel in uninhibited and inhibited acid solutions containing 200 ppm concentrations of cefradine are presented in Figure 2a. EIS spectra obtained consists of one depressed capacitive loop (one time constant in Bode-phase plot). The increased diameter of capacitive loop obtained in 1 M HCl in presence of cefradine indicated the inhibition of corrosion of mild steel. The high frequency capacitive loop may be attributed to the charge transfer reaction.

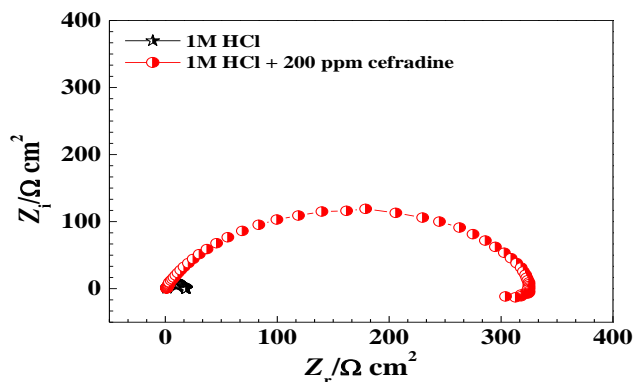


Figure 2a. Nyquist plots in absence and presence of 200 ppm concentration of cefradine

Corrosion kinetic parameters derived from EIS measurements and inhibition efficiencies are given in Table 1. Double layer capacitance (C_{dl}) and charge transfer resistance (R_{ct}) were obtained from EIS measurements as described elsewhere [26]. It is apparent from Table 1 that the impedance of the inhibited system amplified with the inhibitor the C_{dl} values decreased with inhibitor. This decrease in C_{dl} results from a decrease in local dielectric constant and/or an increase in the thickness of the double layer, suggested that inhibitor molecules inhibit the iron corrosion by adsorption at the metal/acid interface [27]. The depression in Nyquist semicircles is a feature for solid electrodes and often referred to as frequency dispersion and attributed to the roughness and other inhomogeneities of the solid electrode [28]. In this behaviour of solid electrodes, the parallel network: charge transfer resistance-double layer capacitance is established where an inhibitor is present. For the description of a frequency independent phase shift between an applied ac potential and its current response, a constant phase element (CPE) is used which is defined in impedance representation as in Eqn. (6)

$$Z_{CPE} = Y_0^{-1} (i\omega)^{-n} \tag{6}$$

where, Y_0 is the CPE constant, ω is the angular frequency (in rad s^{-1}), $i^2 = -1$ is the imaginary number and n is a CPE exponent which can be used as a gauge of the heterogeneity or roughness of the surface [29]. Depending on the value of n , CPE can represent resistance ($n = 0, Y_0 = R$), capacitance ($n = 1, Y_0 = C$), inductance ($n = -1, Y_0 = L$) or Warburg impedance ($n = 0.5, Y_0 = W$).

Figure 2b showed the electrical equivalent circuit employed to analyse the impedance spectra. Excellent fit with this model was obtained for all experimental data.

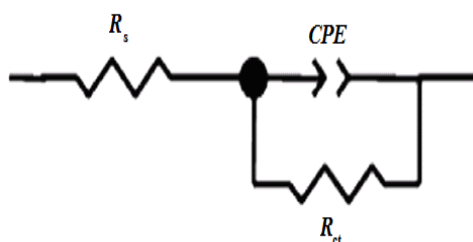


Figure 2b electrochemical equivalent circuit used to fit the impedance measurements that include a solution resistance (R_s), a constant phase element (CPE) and a polarization resistance or charge transfer (R_{ct})

The electrochemical parameters, including R_s , R_{ct} , Y_0 and n , obtained from fitting the recorded EIS data using the electrochemical circuit of Figure 3 are listed in Table 1. C_{dl} values derived from CPE parameters according to Eqn. (7) are listed in Table 1.

$$C_{dl} = (Y_0 \cdot R_{ct}^{1-n})^{1/n} \quad (7)$$

Table 1. Impedance parameters and inhibition efficiency values for mild steel after 30 min immersion period in 1 M HCl in absence and presence of 200 ppm of cefradine

Inhibitor	Conc. (ppm)	R_s ($\Omega \text{ cm}^2$)	R_{ct} ($\Omega \text{ cm}^2$)	C_{dl} ($\mu\text{F cm}^{-2}$)	$E\%$
Cefradine	-	1.07	17	62	-
	200	0.88	324	42	94.7

3.2 Potentiodynamic polarization measurements

Polarization measurements were carried out in order to gain knowledge concerning the kinetics of the cathodic and anodic reactions. Figure 3 presented the results of the effect of cefradine on the cathodic and anodic polarization curves of mild steel in 1 M HCl, respectively. It could be observed that both the cathodic and anodic reactions were suppressed with the addition of cefradine, which suggested that the cefradine reduced anodic dissolution and also retarded the hydrogen evolution reaction. Electrochemical corrosion kinetics parameters, i.e. corrosion potential (E_{corr}), cathodic and anodic Tafel slopes (b_a , b_c) and corrosion current density (I_{corr}) obtained from the extrapolation of the polarization curves, were given in Table 2.

Table 2. Potentiodynamic polarization parameters for mild steel in absence and presence of 200 ppm cefradine in 1 M HCl

Inhibitor	Conc. (ppm)	Tafel data				Linear polarization data		
		E_{corr} (mV vs. SCE)	I_{corr} ($\mu\text{A cm}^{-2}$)	b_a (mV dec ⁻¹)	b_c (mV dec ⁻¹)	$E\%$	R_p ($\Omega \text{ cm}^2$)	$E\%$
Cefradine	-	-469	731	73	127	-	17.2	-
	200	-491	66	84	153	91	321	95

The parallel cathodic Tafel curves in Figure 3 suggested that the hydrogen evolution is activation-controlled and the reduction mechanism is not affected by the presence of the inhibitor. The region between linear part of cathodic and anodic branch of polarization curves becomes wider as the inhibitor is added to the acid solution. Similar results were found in the literature [30]. The values of b_c changed with increasing inhibitor concentration, indicated the influence of the compounds on the kinetics of hydrogen evolution. Investigation of Table 2 revealed that the values of b_a change slightly in the presence of Cefradine where as more pronounced change occurs in the values of b_c , indicating

that both anodic and cathodic reactions are affected but the effect on the cathodic reactions is more prominent. Due to the presence of some active sites, such as aromatic rings, hetero-atoms in the studied compound for making adsorption, they may act as adsorption inhibitors. Being absorbed on the metal surface, these compounds controlled the anodic and cathodic reactions during corrosion process, and then their corrosion inhibition efficiencies are directly proportional to the amount of adsorbed inhibitor. The functional groups and structure of the inhibitor play important roles during the adsorption process. On the other hand, an electron transfer takes place during adsorption of the neutral organic compounds at metal surface [31]. As it can be seen from Table 2, the studied inhibitor reduced both anodic and cathodic currents with a slight shift in corrosion potential (22 mV). According to Ferreira and others [32, 33], if the displacement in corrosion potential is more than 85mV with respect to corrosion potential of the blank solution, the inhibitor can be seen as a cathodic or anodic type. In the present study, the displacement was 22 mV which indicated that the studied inhibitor is mixed-type inhibitor. The results obtained from Tafel polarization showed good agreement with the results obtained from EIS.

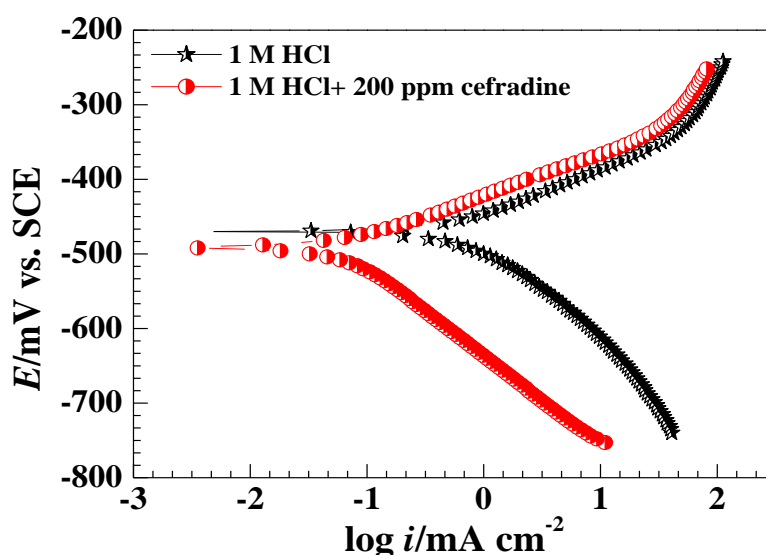


Figure 3. Typical polarization curves for corrosion of mild steel in 1 M HCl in the absence and presence of 200 ppm concentration of cefradine

3.3. Linear polarization resistance

Polarization resistance values were determined from the slope of the potential–current lines,

$$R_p = A \frac{dE}{dI} \quad (8)$$

where A is surface area of electrode, dE is change in potential and dI is change in current. The inhibition efficiencies and polarization resistance parameters are presented in Table 2. The results

obtained from Tafel polarization and EIS showed good agreement with the results obtained from linear polarization resistance.

3.6 Weight loss measurement

3.6.1 Effect of inhibitor concentration

Figure 4a showed the trend of inhibition efficiencies obtained from weight loss measurements for different concentrations of cefradine in 1 M HCl after 3 h immersion at 308 K. The inhibition efficiency increased up to 200 ppm concentration of inhibitor and thereafter almost stable.

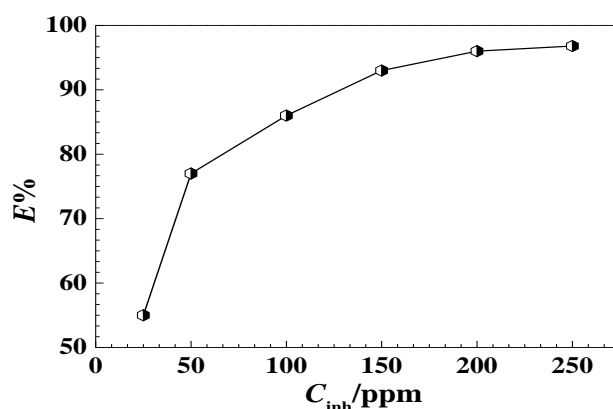


Figure 4a Variation of inhibition efficiency with concentration of inhibitor

3.6.2 Effect of immersion time

The effect of increasing time on the efficiency of cefradine is shown in Figure 4b. At 200 ppm, increasing immersion time resulted in increase in efficiency upto 18 h but thereafter consistent inhibition efficiency. The consistent inhibition efficiency can be attributed to the presence of persistent film of inhibitor on mild steel surface.

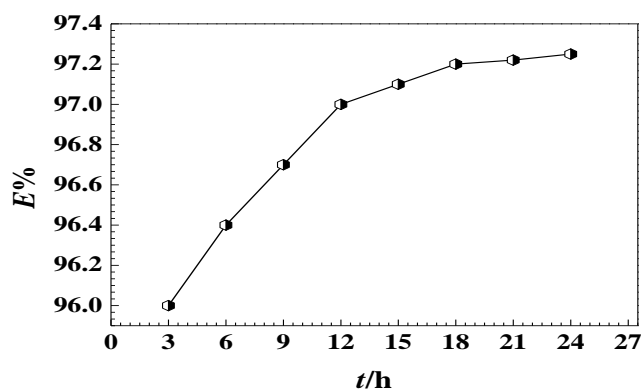


Figure 4b Variation of inhibition efficiency with immersion time, t

3.6.4 Effect of temperature

The effect of temperature on the performance of the inhibitor at a concentration of 200 ppm for mild steel in 1 M HCl at 308, 318, 328 and 338 K was studied using weight loss measurements as shown in Figure 4c. The corrosion rate increased with increasing temperature both in free and inhibited acid. It could be seen that cefradine had good inhibition efficiency ($E\%$) against corrosion of mild steel in HCl solution, but, decreased with increasing temperature, which suggested that corrosion inhibition of mild steel by cefradine caused by the adsorption of inhibitor molecule while higher temperatures caused the desorption of cefradine from the mild steel surface [5].

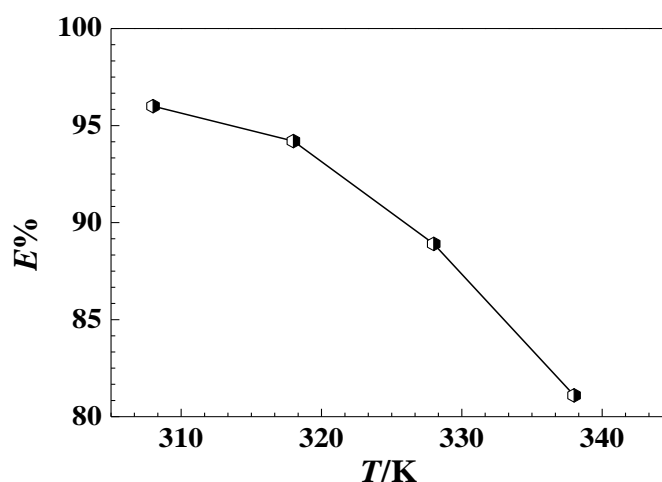


Figure 4c Variation of inhibition efficiency with temperature of the solution

3.7 Activation Parameters and adsorption isotherm

It has been reported by number of authors [34, 35] that in acid solution, logarithm of the corrosion rate is a linear function with $1/T$ (Arrhenius equation):

$$\log C_R = \frac{-E_a}{2.303RT} + \lambda \quad (9)$$

Where, E_a is the apparent activation energy, R general gas constant and λ is the Arrhenius pre exponential factor. A plot of log of corrosion rate obtained by weight loss measurement versus $1/T$ gave straight line as shown in Figure 5a. The values of activation energy obtained from the slope of the lines are given in Table 2.

An alternative formula of the Arrhenius equation is the transition state equation [36]:

$$C_R = \frac{RT}{Nh} \exp\left(\frac{\Delta S^*}{R}\right) \exp\left(-\frac{\Delta H^*}{RT}\right) \quad (10)$$

Where, h is plank's constant, N the Avogadro's number, ΔS^* the entropy of activation and ΔH^* the enthalpy of activation. A plot of $\log(C_R/T)$ versus $1/T$ gave a straight line (Figure 5b), with a slope of $(-\Delta H^*/2.303R)$ and an intercept of $[\log(R/Nh) + (\Delta S^*/2.303R)]$, from which the values of ΔS^* and ΔH^* were calculated and listed in table 2. The data shows that thermodynamic activation

functions (E_a) of the corrosion in mild steel in 1M HCl solution in the presence of the inhibitor is higher than those in free acid solution indicating that all the inhibitors lowers the inhibition efficiency at higher temperature [36, 37]. The positive signs of enthalpy (ΔH^*) reflect the endothermic nature of dissolution process. The shift towards positive value of entropy(ΔS^*) imply that the activated complex in the rate determining step represents dissociation rather than association, meaning that disordering increases on going from reactants to the activated complex.

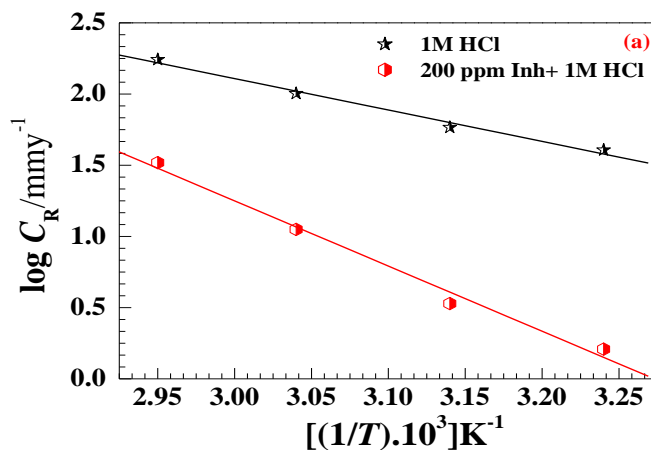


Figure 5a. Arrhenius plot for $\log C_R$ vs. $1/T$

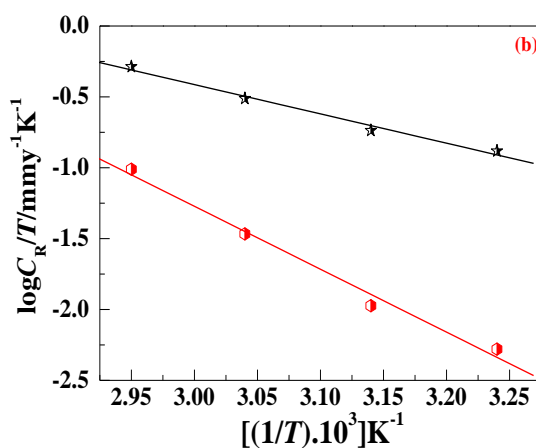


Figure 5b. Transition state plot for $\log C_R/T$ vs. $1/T$

The degree of surface coverage (θ) for different inhibitor concentrations was evaluated from weight loss measurements. The best correlation between the experimental results and isotherm functions was obtained using Langmuir adsorption isotherm. The Langmuir isotherm for monolayer chemisorption is given by the following equation [38]:

$$\frac{C_{inh}}{\theta} = \frac{1}{K_{ads}} + C_{inh} \tag{11}$$

where, K_{ads} is the equilibrium constant of the adsorption/desorption process. The plots of C_{inh}/θ vs. C_{inh} yield straight line with nearly unit slope showing that the adsorption of CFD can be fitted to Langmuir adsorption as presented in Figure 6.

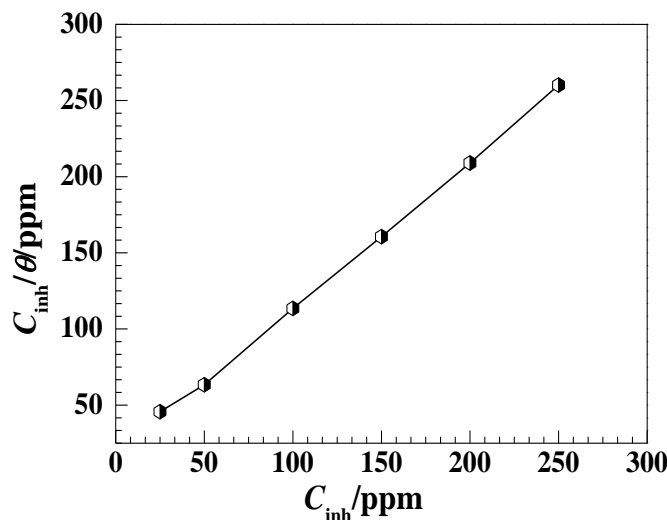
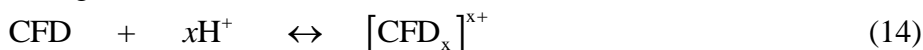


Figure 6. Langmuir adsorption isotherm

4. MECHANISM OF INHIBITION

The inhibition efficiency of cefradine against the corrosion of mild steel in 1 M HCl can be explained on the basis of the number of adsorption sites, molecular size and mode of interaction with the metal surface [35, 38]. Physical adsorption requires presence of both electrically charged surface of the metal and charged species in the bulk of the solution; the presence of a metal having vacant low-energy electron orbital and of an inhibitor with molecules having relatively loosely bound electrons or heteroatoms with lone pair electrons. However, the compound reported is an organic base which can be protonated in an acid medium. Thus they become cations, existing in equilibrium with the corresponding molecular form



The protonated cefradine, however, could be attached to the mild steel surface by means of electrostatic interaction between Cl^- and protonated cefradine since the mild steel surface has positive charge in the HCl medium [5]. This could further be explained based on the assumption that in the presence of Cl^- , the negatively charged Cl^- would attach to positively charged surface. When cefradine adsorbs on the mild steel surface, electrostatic interaction takes place by partial transference of electrons from the polar atom (N atom and delocalized π -electrons of the aromatic ring) of cefradine to the metal surface.

5. CONCLUSIONS

The following main conclusions are drawn from the present study:

1. Cefradine was found to be a good inhibitor for mild steel corrosion in acid medium.
2. The inhibition efficiency of cefradine decreased with temperature, which leads to an increase in activation energy of the corrosion process.
3. Potentiodynamic polarization curves revealed that cefradine is a mixed-type inhibitor

ACKNOWLEDGEMENT

One of the authors A. K.S. is thankful to NWU, South Africa for financial assistance.

References

1. G. E. Badr, *Corros. Sci.* 51 (2009) 2529-
2. Y. Ren, Y. Luo, K. Zhang, G. Zhu, X. Tan, *Corros. Sci.* 50 (2008) 3147-
3. K. S. Jacob, G. Parameswaran, *Corros. Sci.* 52 (2010) 224-228
4. S. A. Abd El-Maksoud, A. S. Fouda, *Mater Chem Phys* 93 (2005) 84-
5. A. K. Singh, M. A. Quraishi, E. E. Ebenso, *Int. J. Electrochem. Sci.* 6 (2011) 5676-5688
6. M. Behpour, S. M. Ghoreishi, N. Soltani, M. Salavati-Niasari, M. Hamadani, A. Gandomi, *Corros. Sci.* 50 (2008) 2172-2181
7. A. K. Singh, M. A. Quraishi, *Corros. Sci.* 51 (2009) 2752-2760.
8. A. K. Singh, M. A. Quraishi, *Corros. Sci.* 52 (2010) 152-160.
9. A. K. Singh, M. A. Quraishi, *Corros. Sci.* 52 (2010) 1529-1535.
10. A. Asan, S. Soylu, T. Kiyak, F. Yildirim, S. G. Oztas, N. Ancin, M. Kabasakaloglu, *Corros. Sci.* 48 (2006) 3933-3944.
11. M. Lebrini, F. Bentiss, H. Vezin, M. Lagrenee, *Corros. Sci.* (2006) 1279-1291
12. J. Aljourani, K. Raieisi, M. A. Golozar, *Corros. Sci.* 51 (2009) 1836-1843
13. M. Lebrini, M. Traisnel, M. Lagrenee, B. Mernari, F. Bentiss, *Corros. Sci.* 50 (2008) 473-479
14. B. B. Damaskin, A. N. Frumkin, N. S. Hush (Ed.) Adsorption of molecules on electrodes, Wiley-Interscience, London, (1971) p. 1.
15. M. A. Quraishi, M. Z. A. Rafiquee, Sadaf Khan, Nidhi Saxena. *J. Appl. Electrochem.*, 37 (2007) 1153-
16. A. Popova, E. Sokolova, S. Raicheva, M. Christov, *Corros. Sci.* 45 (2003) 33-58
17. A. K. Singh, M. A. Quraishi, E. E. Ebenso, *Int. J. Electrochem. Sci.* 6 (2011) 5676-5688
18. A. K. Singh, M. A. Quraishi, *Mater. Chem. Phys.* 123 (2010) 666-677
19. A. K. Singh, E. E. Ebenso, M. A. Quraishi, *Int. J. Electrochem. Sci.* 7 (2012) 2320-2333
20. A. K. Singh, E. E. Ebenso, *Int. J. Electrochem. Sci.* 7 (2012) 2349-2360
21. G. Moretti, F. Guidi, G. Grion, *Corros. Sci.* 46, (2004) 387-403
22. F. C. Giacomelli, C. Giacomelli, M. F. Amadori, V. Schmidt, A. Spinelli, *Mater. Chem. Phys.* 83, (2004) 124-
23. E. S. Ferreira, C. Giacomelli, F. C. Giacomelli, A. Spinelli, *Mater. Chem. Phys.* 83 (2004) 29-
24. E. E. F. El Sherbini, *Mater. Chem. Phys.* 61, (1999) 223-
25. M. S. Morad, *Corros. Sci.* 50 (2008) 436-448
26. A. K. Singh, M. A. Quraishi, *Corros. Sci.* 52 (2010) 1373-1385
27. F. Bentiss, C. Jama, B. Mernari, H. E. Attari, L. E. Kadi, M. Lebrini, M. Traisnel, M. Lagrenee, *Corros. Sci.* 51 (2009) 1628-1635.
28. H. Ashassi-Sorkhabi, D. Seifzadeh, M. G. Hosseini, *Corros. Sci.* 50 (2008) 3363-3370.

29. A. Popova, M. Christov, *Corros. Sci.* 48 (2006) 3208-3221
30. A. K. Singh, M. A. Quraishi, *J. Mater. Environ. Sci* 1 (2010) 101-110
31. M.S. Morad, A.M. Kamal El-Dean, *Corros. Sci.* 48 (2006) 3398
32. E.S. Ferreira, C. Giancomelli, F.C. Giacomelli, A. Spinelli, *Mater. Chem. Phys.* 83 (2004) 129,
33. W.H. Li, Q. He, C.L. Pei, B.R. Hou, *J. Appl. Electrochem.* 38 (2008) 289
34. A. K. Singh, *Ind. Engg. Chem. Res.* 51 (8), 3215-3223
35. A. K. Singh, M. A. Quraishi, *Int. J. Electrochem. Sci* 7, 3222-3241
36. A. K. Singh, M. A. Quraishi, *J. Appl. Electrochem.* 40 (2010) 1293-1306
37. G. Mu, X. Li, G. Liu, *Corros. Sci.* 47 (2005) 1932-1952
38. A. K. Singh, M. A. Quraishi, *J. Appl. Electrochem.* 41 (1), 7-18